nature communications

Article

https://doi.org/10.1038/s41467-026-69647-y

Siderophore-producing Bacillus and free-living nematodes are associated with soil suppressiveness to banana root-knot nematodes

Received: 20 November 2024

Accepted: 5 February 2026

Published online: 12 February 2026

Check for updates

Qiaofang Lu[1,2,6], Kunguang Wang[1,6], Shaohua Gu[1,6] ✉, Jing Ma[1], Dongming Cui[1], Zhiguang Chi[1], Baoshen Li[1], Xiaoyu Zai[1], Nanqi Wang[1], Tianqi Wang[1], Zhechao Dou[1], Fusuo Zhang[1], Stefan Geisen[3], Jos M. Raaijmakers[4,5], Chunxu Song[1] ✉ & Yuanmei Zuo[1] ✉

The control of soil-borne diseases is crucial for ensuring global food security. Here, we investigate the impact of the root-knot nematode (*Meloidogyne*) on banana continuous cropping over a period of 11 years. The results show significant root infestation initially, but disease incidence declined markedly from the 7th cropping year onwards. Soil community profiling revealed that this intriguing onset of nematode suppressiveness was associated with changes in free-living nematode populations and rhizosphere microbiome composition. Rhizosphere microbiome analyses and strain isolation pinpointed *Bacillus velezensis* as a keystone taxon in soil suppressiveness to *Meloidogyne*. Genomics, metabolomics and bioassays validated the suppressive effects of *B. velezensis* against *Meloidogyne* and identified the siderophore bacillibactin as key metabolite with repellent and nematicidal activities. By integrating long-term field studies with multi-omics approaches, this study uncovered co-occurring increases in specific rhizobacterial genera and free-living nematodes associated with reduced root-parasitic nematode populations, offering valuable insights for sustainable agriculture.

Soil-borne diseases pose a persistent and escalating threat to global food security, particularly under intensive agricultural systems[1,2]. Among soil-borne pathogens, plant parasitic nematodes (PPNs) are especially destructive, accounting for an estimated 10% loss in global crop yields annually[1,3,4]. This problem is exacerbated by the widespread practice of continuous cropping where the repeated cultivation of a single crop leads to the buildup of soil pathogens, including PPNs[5–7]. For example, continuous monoculture of banana (*Musa*) frequently results in the proliferation of root-knot nematodes, notably those from the genus *Meloidogyne*, which cause substantial yield losses[8]. Current management practices rely heavily on chemical nematicides[8–10]. However, their environmental and ecological consequences have spurred urgent calls for more sustainable alternatives.

[1]College of Resources and Environmental Sciences, State Key Laboratory of Nutrient Use and Management (SKL-NUM), National Academy of Agriculture Green Development, China Agricultural University, Beijing, China. [2]Guangxi Key Laboratory for Agro-Environment and Agro-Products Safety, College of Agriculture, Guangxi University, Nanning, China. [3]Laboratory of Nematology, Wageningen University and Research, Wageningen, The Netherlands. [4]Department of Microbial Ecology, Netherlands Institute of Ecology, Wageningen, The Netherlands. [5]Institute of Biology, Leiden University, Leiden, the Netherlands. [6]These authors contributed equally: Qiaofang Lu, Kunguang Wang, Shaohua Gu. ✉e-mail: gsh2025@cau.edu.cn; chunxu.song@cau.edu.cn; zuoym@cau.edu.cn

One promising avenue is the exploitation of natural disease-suppressive soils, where native soil microbiota suppresses pathogens without the need for external inputs. These suppressive effects often emerge over time during continuous cropping, particularly following early disease outbreaks[6,11]. Suppressive soils are typically characterized by the enrichment of specific microbial taxa in the rhizosphere that interfere with key stages in the pathogen's life cycle[12–14]. For example, genera such as *Pseudomonas*, *Purpureocillium* and *Pochonia* have been implicated in the biological suppression of soybean cyst nematodes[6]. Several root-knot nematode-suppressive soils have been found in nature, most studies are not focused on those formed under long-term nematode infestation in continuous cropping conditions[15]. Numerous microbial strains isolated from nematode-suppressive soils and have been well investigated and commercialized[16,17]. However, despite the identification of some antagonistic microbial genera[18–20], the mechanistic understanding of microbiome-mediated suppression of *Meloidogyne* under long-term monoculture remains largely elusive. In particular, the multipartite interactions between the rhizosphere microbiome, other soil microbiota and *Meloidogyne* have received little attention.

To address this knowledge gap, we monitored a long-term banana monoculture system as a model to uncover the (micro)biological mechanisms underlying natural suppression of *Meloidogyne*-induced root-knot disease. To unravel the key players associated with induced suppressiveness to root-knot disease, we focused our analyses on the putative roles of free-living nematodes (FLNs, including bacterivores, fungivores, and omnivore-predators) and the banana rhizosphere microbiome. FLNs can enhance plant performance by increasing carbon and nutrient cycling and suppressing plant pathogens, making most FLNs beneficial to plants[21,22]. FLNs are also considered non-target organisms in PPN control, with *Caenorhabditis elegans* being a prominent member that is widely used as a biological model for soil toxicity studies[23]. Considering the crucial role of the microbiome in plant fitness and disease control, we hypothesize that prolonged continuous cropping reshapes both the nematode community and the rhizosphere microbiome, leading to increased abundance of FLNs and specific microbial taxa with complementary suppressive activities.

To test our hypothesis, we examined a long-term (11 years) field trial, tracking the incidence of root-knot nematode disease over time (Fig. 1). We combined phenotypic assessments of disease incidence and high-throughput sequencing to analyze changes in soil nematode community and banana rhizosphere microbiome. Our results revealed a significant decline in disease incidence after the 7th year, coinciding with shifts in FLNs diversity and enrichment of *Bacillus* species in the rhizosphere. Further isolation and functional validation demonstrated that *Bacillus velezensis* was a keystone taxon in disease suppression, with the siderophore bacillibactin identified as a key metabolite exhibiting both repellent and nematicidal effects on *Meloidogyne*. Importantly, bacillibactin showed minimal toxicity to *C. elegans*, underscoring its potential as a selective biocontrol agent. Together, our findings highlight evidence of root-knot nematode suppression through the synergistic effect of free-living nematodes and siderophore-secreting rhizobacteria. Our study advances the understanding of microbiome-mediated soil suppressiveness and offers eco-friendly strategies for sustainable nematode management in intensive cropping systems.

Results

Induction of suppressiveness to root-knot nematode disease during continuous banana cropping

To determine the effect of different cropping times on banana root-knot nematode disease occurrence, we collected the samples from four groups of banana plantations with continuous cropping for 1 (Y1), 4 (Y4), 7 (Y7), and 10 years (Y10) in 2016; 2 (Y2), 5 (Y5), 8 (Y8), and 11 (Y11) years in 2017, and investigated root-knot nematode disease incidence (Fig. 1a and Fig. 2a). Root-knot nematode disease incidence showed a parabolic pattern, peaking at 90–96% in plantations of 2, 4, and 5 years of age (Y2, Y4, Y5), followed by a significant decline to 40–50% after 7, 8, 10 and 11 years (Y7, Y8, Y10, Y11). A similar trend was observed for gall index results (Fig. 2b, c). Although different sets of cropping years were sampled in 2016 and 2017, combining the data showed consistent patterns in disease incidence across years, supporting the robustness of the space-for-time substitution design. Total soil nematode abundance displayed a concomitant increase during continuous banana cultivation, with the lowest levels observed in Y1 and Y2 (approximately 1800 individuals per 100 g dry soil), while in Y11 the highest nematode abundances existed, approximately 4 times higher than in Y1 and Y2 (Fig. 2d). Collectively, these results show outbreaks of root-knot nematode disease of banana in the first 5 years of continuous cropping, followed by a decline in disease incidence and gall index from year 7 onwards.

Association of free-living soil nematode abundance and root-knot suppressiveness

To investigate the potential involvement of soil nematode abundance and community structure in induced suppressiveness to root-knot disease of banana caused by *Meloidogyne*, we integrated morphological assessments (in 2016, including Y1, Y4, Y7, and Y10) and high-throughput sequencing (in 2017, including Y2, Y5, Y8, and Y11) (Fig.1a). For the results in 2016, we observed that the Shannon index was lower in Y1 compared to Y4, Y7, and Y10, indicating a continuous cropping effect on nematode α diversity (Fig. 3a). Unconstrained principal coordinate analysis (PCoA) showed that long-term continuous banana cropping significantly influenced soil nematode communities in 2016 (Adonis; $R^2 = 0.41$; $p < 0.001$) and in 2017 (Adonis; $R^2 = 0.38$; $p < 0.001$), with a distinct separation between short-term and long-term cropping (Fig. 3b and Supplementary Fig. 1a).

Analysis of nematode trophic groups in 2016 revealed that plant-parasites (Pp) increased in relative abundance from 13.9% in year 1 (Y1) to 50.5% in year 4 (Y4), then decreased to 37.5% in year 7 (Y7) and 30.9% in year 10 (Y10) (Fig. 3c). Among the FLNs (putatively beneficial nematodes), bacterivores (Ba) were most abundant in Y1 at 73.6% while decreasing to 30–40% in subsequent cropping times; the relative abundance of fungivores (Fu) increased with continuous cropping, rising from 8.4% in Y1 to nearly 20% in Y7 and Y10, omnivores-predators (OP) showed similar changes, increasing from 3.8% in Y1 to nearly 11% in Y7 and Y11 (Fig. 3c).

The relative abundance of *Meloidogyne* showed a similar trend with Pp, increasing from 2% in Y1 to 6.5% in Y4 and decreasing to 1.3% in Y10 (Fig. 3d). Under the 18S rRNA amplicon sequencing results, we also found that *Meloidogyne* was most abundant in Y2 and Y5 at 8.0-13.0%, while decreasing to 0.1-1% in Y8 and Y11 (Supplementary Fig. 1b). Combining the nematode trophic groups with *Meloidogyne* relative abundance, a significant positive association was found between the *Meloidogyne* relative abundance and Pp relative abundance (Pearson's $r = 0.63$, $p < 0.001$), whereas negative associations were observed between *Meloidogyne* relative abundance and Fu relative abundance (Pearson's $r = -0.52$, $p = 0.0029$) and OP relative abundance (Pearson's $r = -0.47$, $p = 0.0083$). No significant association was found between *Meloidogyne* relative abundance and Ba relative abundance (Pearson's $r = -0.2$, $p = 0.29$) (Fig. 3e). Collectively, these results indicated that long-term continuous banana cropping is associated with a compositional shift in the soil nematode community, with a reduced abundance of PPNs (especially *Meloidogyne*) and an increase in abundance of FLNs (especially Fu and OP).

Long-term continuous cropping enriches specific rhizobacterial genera with *Bacillus* as a key taxon

To explore the putative effects of the banana root microbiome on root-knot nematode disease during continuous banana cropping, we

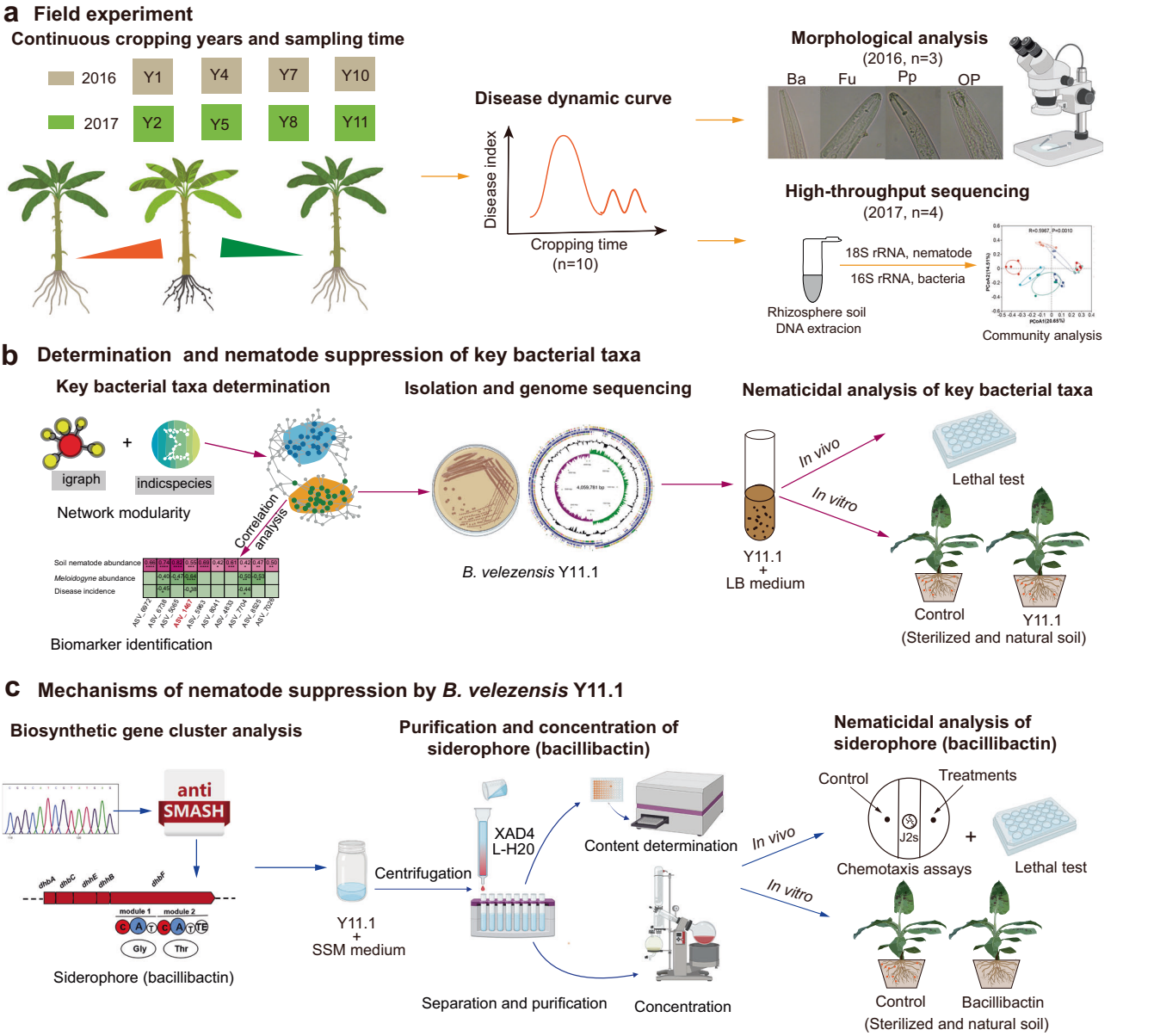

Fig. 1 | An overview of the experimental workflow for this study. a Field investigation and sampling. Four groups of banana plantations were selected for sampling in 2016 and 2017. Disease index was determined by combining the samples in 2016 and 2017. Soil nematodes were identified by morphological assessments (2016; including Y1, Y4, Y7, and Y10) and high-throughput sequencing (2017; including Y2, Y5, Y8, and Y11), total DNA was isolated from rhizosphere soil in 2017 to analyze nematode and bacterial community. **b** Determination, isolation, and identification of key bacterial taxa. The in vivo and in vitro experiments were used to analyze the nematicidal effects of key bacterial taxa. **c** Mechanisms of nematode suppression by key bacterial taxa. The siderophore bacillibactin was determined as the potential nematicidal compound, after purifying and concentrating the siderophore bacillibactin, nematode suppression effects were determined by the chemotaxis assays, lethal test and pot experiments. Created in BioRender. Wang, K. (2026) https://BioRender.com/m3rcb3k.

investigated the changes in abundance and community structure of rhizosphere bacteria (Fig. 1b). Results of *16S rRNA* gene amplicon sequencing showed that the bacterial community composition of the banana rhizosphere changed during continuous banana cropping with significantly higher diversity in Y5, Y8, and Y11 (7.9–8.0 of Shannon index and 4324–4382 of Chao1) compared to Y2 (7.7 of Shannon index and 3581 of Chao1) (Fig. 4a). Consistent changes were observed in bacterial copy numbers, which increased with continuous cropping, reaching the highest abundance of 13.6×10^8 copies per gram of soil in Y11 (Fig. 4b). Moreover, PCoA based on Bray-Curtis distances revealed changes in bacterial community structure with prolonged cropping (Adonis; $R^2 = 0.32$; $p < 0.001$) (Fig. 4c).

Co-occurrence network analyses of 16S amplicon sequence variants (ASVs) detected in the early (Y2, Y5) and late (Y8, Y11) stages of cropping revealed two modules, each associated with relatively high proportions of indicator ASVs, i.e. bacterial taxa that responded most significantly to cropping time (Spearman's $\rho > 0.6$, $p < 0.01$) (Fig. 4d). Notably, ASVs assigned to Y2, Y5 were predominantly located in module 1 (77 ASVs) and distinct from module 2 (117 ASVs), which primarily contained ASVs assigned to Y8 and Y11 (Fig. 4e and Supplementary Data 1). Each module consisted of multiple phyla/genera: Actinobacteriota was more abundant in module 1, whereas Acidobacteriota and Proteobacteria (e.g. genus *Allorhizobium-Neorhizobium-Pararhizobium-Rhizobium*; *Mesorhizobium*) were more abundant in module 2 (Fig. 4f and Supplementary Table 1). Four phyla/genera, including Firmicutes (e.g. genus *Bacillus*), Gemmatimonadota, Myxococcota, and Nitrospirota (e.g. genus *Nitrospira*) exclusively appeared in module 2, whereas Planctomycetota was observed only in

https://doi.org/10.1038/s41467-026-69647-y

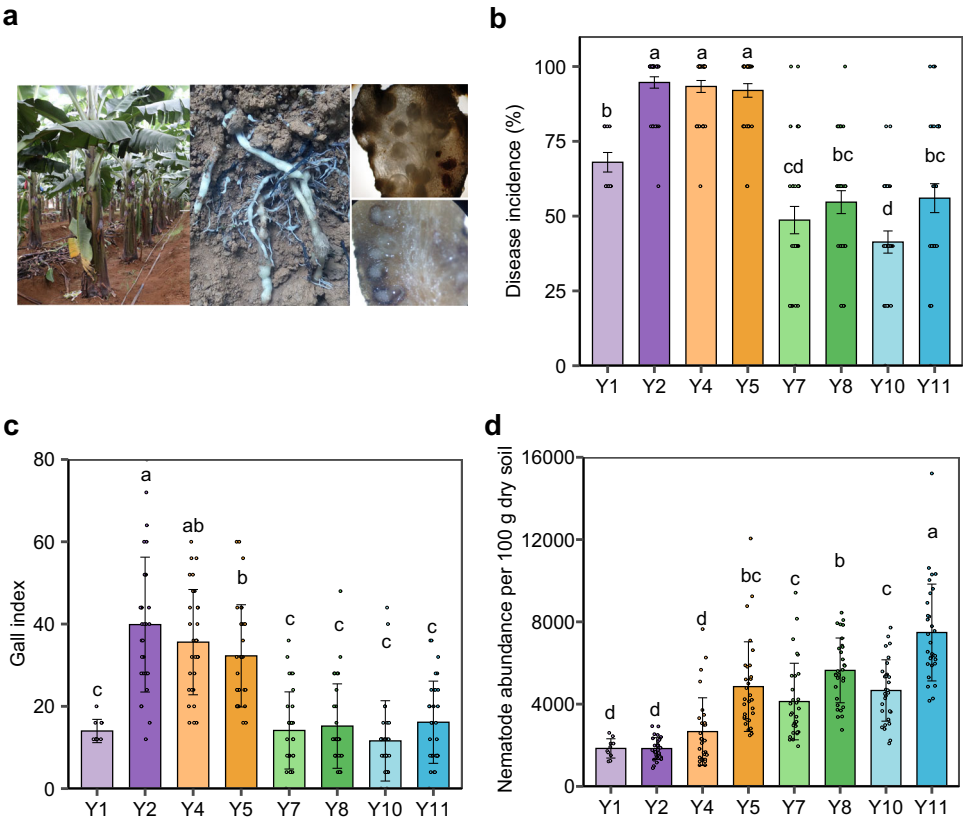

Fig. 2 | The occurrence of root-knot nematode disease during continuous banana cultivation. a, The intensive cropping pattern of banana in our study, and the typical symptoms of root-knot nematode infestation in the field. **b**–**d** The disease incidence (**b**), gall index (**c**), and the soil nematodes abundance (**d**) in banana orchards cultivated continuously for 1 year (Y1), 2 years (Y2), 4 years (Y4), 5 years (Y5), 7 years (Y7), 8 years (Y8), 10 years (Y10) and 11 years (Y11). Data presented as mean ± SD ($n = 10$ biologically independent samples for Y1 and n = 30 biologically independent samples for other cropping times). Statistical differences indicated by distinct lowercase letters ($p \le 0.05$) following LSD test subsequent to one-way ANOVA. Multiple testing corrections are performed by BH algorithm. Two-sided tests were used for alternative hypothesis testing. Exact *p*-values of statistical tests are provided in the Source data file.

module 1 (Fig. 4f and Supplementary Table 1). Positive associations were observed between module 1 and *Meloidogyne* relative abundance (Pearson's $r = 0.4$; $p = 0.023$), whereas significant negative associations were found between module 2 and *Meloidogyne* relative abundance (Pearson's $r = -0.37$; $p = 0.037$) (Fig. 4g).

To identify bacterial taxa potentially involved in root-knot nematode disease suppressiveness, we selected the top 10 ASVs that responded most significantly to the cropping time and were most enriched in Y8 and Y11 as compared to Y2 and Y5. Three specific ASVs (ASV6738, ASV1467, ASV7704) showed significantly negative correlations with *Meloidogyne* relative abundance and disease incidence. Notably, ASV1467 had the strongest negative association (Spearman's $\rho = -0.64$) with *Meloidogyne* relative abundance (Fig. 5a and Supplementary Fig. 2). Independently, we conducted random forest modelling with the indicator ASVs to further predict the potential link between the main ASV predictors of *Meloidogyne* relative abundance. Consistently, the results indicated that the most important predictor of *Meloidogyne* was ASV1467 (9.5%) (Supplementary Fig. 3a). ASV1467 was taxonomically delineated as *Bacillus* and enriched in the banana rhizosphere in Y8 (0.24%) and Y11 (0.27%) as compared to Y2 (0.15%) and Y5 (0.07%) (Fig. 5b). These findings suggest a potential role of ASV1467 in root-knot nematode suppressiveness.

Bacillus velezensis and its siderophore bacillibactin suppress *M. incognita* in banana via repellent and nematicidal activities

To test the protective role of ASV1467 against *M. incognita* in banana, we isolated a total of 190 rhizobacteria. Based on 16S rRNA sequencing of these isolates, strain Y11.1, isolated from banana rhizosphere samples of Y11, had an identical 16S rRNA sequence (451 bp) as ASV1467 (Supplementary Fig. 3b). We then sequenced the genome of *Bacillus* sp. Y11.1 and whole-genome phylogenetic analyses revealed that strain Y11.1 belongs to the *B. velezensis* group (Fig. 5c and Supplementary Fig. 4). Subsequent in vitro assays showed that *B. velezensis* Y11.1 exhibited lethal effect on *M. incognita*, with relative mortality rates reaching 69.72% at 48 h (Supplementary Fig. 5).

To experimentally validate that *B. velezensis* Y11.1 can suppress root-knot nematodes in soil, we conducted two greenhouse experiments (Fig.1b and Fig. 5d). When banana plants were cultivated in sterilized soil, a treatment with cell suspensions of *B. velezensis* Y11.1 promoted banana growth and significantly decrease in *M. incognita* infection and reproduction (Fig. 5e and Supplementary Fig. 6a). Gall and egg mass numbers were reduced by 46.2% and 69.6%, respectively. Similar outcomes were found under natural field soil conditions, with *B. velezensis* Y11.1 reducing galls numbers by 59.4%, while enhancing abundance of total soil nematodes by 45.6% and promoting banana growth (Fig. 5f and Supplementary Fig. 6b). Quantitative PCR analysis confirmed a significant reduction in *Meloidogyne* density in soil treated with *B. velezensis* Y11.1 by 48.7%. While *B. velezensis* Y11.1 application to natural soil significantly reduced RKN density, it concurrently increased total nematode abundance due to the proliferation of non-parasitic trophic groups. Thus, the apparent increase in total nematodes does not reflect an increase in RKN, but rather the selective suppression of the pathogen alongside enrichment of free-living nematodes. Our results affirm the suppressive effect of *B. velezensis* Y11.1 against *M. incognita* in banana plants and its ability to promote banana growth.

https://doi.org/10.1038/s41467-026-69647-y

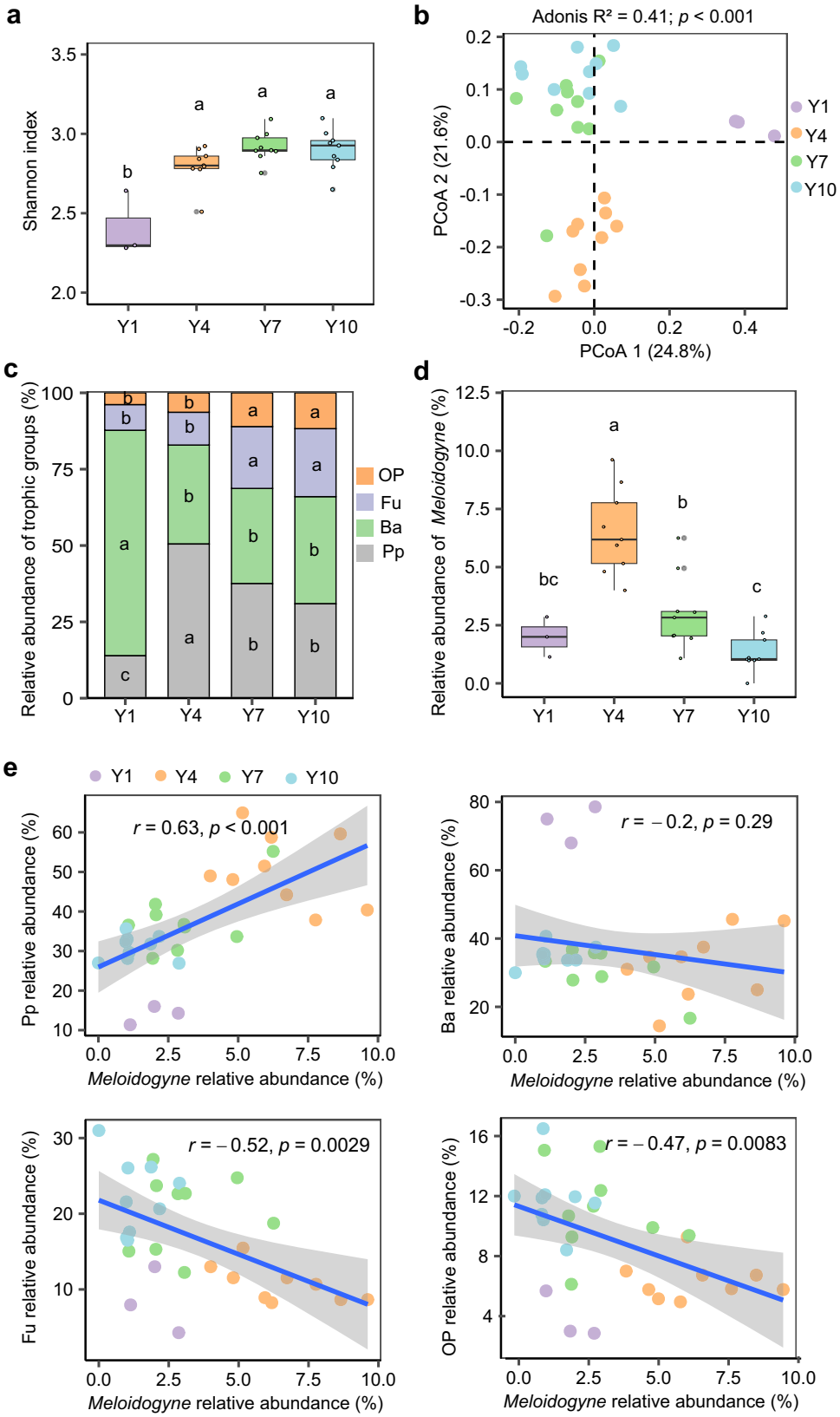

To further identify which metabolites from *B. velezensis* Y11.1 inhibit *M. incognita*, genome mining revealed several secondary metabolites biosynthetic gene clusters (BGCs), including 13 BGCs associated with the biosynthesis of non-ribosomal peptides, polyketides, terpenes, and post-translationally modified peptides (RiPPS). Based on earlier discoveries highlighting potent nematode-suppressive attributes of siderophores[24,25], we focused on the siderophores produced by *B. velezensis* Y11.1 (Fig. 1c). We experimentally showed that Y11.1 supernatants from iron-limited culture conditions (containing siderophore(s)) caused 21.6% more mortality than supernatants from iron-rich culture conditions (without siderophore) (Fig. 6a), suggesting lethal effects of Y11.1 siderophore(s) on

Fig. 3 | The community structure of soil nematodes during long-term continuous banana cultivation. a The Shannon index reflect soil nematode diversity changes. **b** Principal coordinates analysis of the soil nematodes in various cropping banana orchards based on Bray-Curtis distance. **c** Nematode trophic groups in different continuous cropping times of banana. **d** Relative abundance of *Meloidogyne* in banana plantations subjected to continuous cropping for 1 year (Y1), 4 years (Y4), 7 years (Y7), and 10 years (Y10). **e** Pearson correlation analysis between the *Meloidogyne* relative abundance and Pp, Ba, Fu, and OP nematode relative abundance. Shading associated with lines in the panel indicates a 95% confidence interval. For (**a**) and (**d**), boxplot center lines show the median, boxplot bounds show the first quartile Q1 and the third quartile Q3, and whiskers show 1.5 (Q3-Q1) below and above Q1 and Q3, and black dots represent outliers and open dots represent individual values (n = 3 biologically independent samples for Y1 and n = 9 biologically independent samples for other cropping times). Statistical differences indicated by distinct lowercase letters ($p \leq 0.05$) following the LSD test subsequent to one-way ANOVA. Multiple testing corrections are performed by BH algorithm. Two-sided tests were used for alternative hypothesis testing. Ba bacterivores, Fu fungivores, Pp plant-parasites, OP omnivores/predators. Exact *p*-values of statistical tests are provided in the Source data file.

Meloidogyne juveniles. Next, we directed our attention specifically to bacillibactin, a catecholate-type siderophore predicted for one of the BGCs identified in the Y11.1 genome (Supplementary Fig. 7a). The supernatant of Y11.1 cultivated in iron-limited SSM broth, contained 54.7 μM bacillibactin (Supplementary Fig. 7b, c). We next examined the inhibitory effects of bacillibactin on *Meloidogyne*. We found that the purified bacillibactin at 500 μM exhibited lethal effects on *Meloidogyne* juveniles, resulting in relative mortality rates of 11.51% at 48 hrs. In contrast, we found no significant difference in *C. elegans* mortality at various concentrations of bacillibactin compared to the controls (Fig. 6b). We also observed that the Y11.1 supernatant from iron-limited SSM and the purified bacillibactin repelled *Meloidogyne* juveniles: highest chemotaxis indices were found at -0.83 of SSM and -0.30 at 500 μM bacillibactin, respectively (Fig. 6c and Supplementary Fig. 8). In contrast, at concentrations of 50–500 μM, bacillibactin attracted *C. elegans* with an increase in the chemotaxis index from 0.06 to 0.61 (Fig. 6c). To experimentally validate that bacillibactin plays an important role in inhibiting *Meloidogyne* infection of banana roots, we conducted two greenhouse experiments (Fig. 6d). We found that both in sterilized soil and natural soil conditions, adding 40 μmol/kg bacillibactin every 14 days significantly reduced the gall, egg mass numbers, and the nematode abundance in the root, and also promoted banana growth (Fig. 6e, f and Supplementary Fig. 9). These results indicate that the siderophore bacillibactin of *B. velezensis* Y11.1 plays a role in alleviating root-knot nematode infection and reproduction by repelling and causing mortality in *Meloidogyne* juveniles, but attracts the free-living nematode *C. elegans* without causing lethality.

Discussion

Control of soil-borne diseases is essential for the sustainability of agriculture and global food security. However, the mechanisms underlying the suppression of such diseases, particularly those mediated by nematode–microbe interactions often remain unclear. In this study, we demonstrated that long-term continuous banana cropping, while initially exacerbating root-knot nematode (*Meloidogyne*) infestation, led to a marked decline in disease incidence after seven years. This transition toward a disease-suppressive state coincided with a reduced abundance of plant-parasitic nematodes (PPNs), enrichment of free-living nematodes (FLNs), and substantial shifts in the rhizosphere microbiome. Specifically, we discovered that the induction of root-knot disease suppressiveness was accompanied by decreased *Meloidogyne* abundance and enriched *Bacillus* species, where these bacteria mitigate root-knot disease through the secretion of their siderophore bacillibactin. Siderophores (e.g., pyoverdine) have been associated with inhibitory effects for *C. elegans* development, and our study now provides evidence linking bacterial bacillibactin production to root-knot disease suppressiveness (Fig. 6). Our field data demonstrate that suppressive soils are characterized by concurrent enrichment of FLNs and siderophore-producing *Bacillus*. Furthermore, experimental assays with purified bacillibactin confirmed its repellent and nematicidal activity against root-knot nematodes, while showing attraction but no lethal effect on the free-living nematode *C. elegans*. These findings suggest a potential complementary interaction between FLNs and *Bacillus* in shaping soil suppressiveness. However, we note that the current evidence is associative, and a direct mechanistic demonstration of synergistic cross-kingdom interaction remains an important direction for future research. This insight closes a major knowledge gap in the research field of nematode-suppressive soils. Crucially, we show that the uncovered nematode-microbe-plant interaction is essential to mitigation of root-knot disease and further show the mechanisms of co-occurring and potential complementary roles of rhizobacteria and FLNs may provide a fundamental basis to develop strategies for sustainable agriculture and food security.

The phenomenon of disease suppressiveness emerging during continuous monoculture has been reported in several crop-pathogen systems, including take-all disease (*Gaeumannomyces graminis* var. *tritici*) in wheat, root rot (*Rhizoctonia solani*) in sugar beet, *Fusarium* wilt (*Fusarium oxysporum*) in strawberry, and cyst nematode disease (*Heterodera glycine*) in soybean[6,11,26,27]. While various factors—such as crop variety, pathogen diversity, and environmental conditions—can influence the onset and strength of disease suppressiveness, the underlying mechanisms are predominantly (micro)biological in nature. In previous studies, suppressiveness against soybean cyst nematode and wheat take-all disease typically developed after 4 to 6 years of continuous monoculture[6,13], whereas *Fusarium* wilt suppressiveness in strawberry required a minimum of 7 years[27]. In our study, we discovered that root-knot nematode disease in banana initially intensified over the first five years of continuous cultivation but transitioned to a suppressive state from year seven onward. This transition was supported by a significant reduction in PPNs, particularly *Meloidogyne*, and natural suppression properties of *Meloidogyne* may be formed.

The (micro)biological mechanisms underlying natural suppression of disease highlight the importance of rhizosphere biota. Soil nematodes (both PPNs and FLNs) play essential roles in shaping the dynamics of nematode-associated diseases[3,22]. By integrating morphological assessments with high-throughput sequencing, we tracked shifts in soil nematode communities, and both methods consistently revealed a marked decline in *Meloidogyne*, both datasets also showed a clear separation of short-term versus long-term cropping in community structure (Fig. 3 and Supplementary Fig. 1). These convergent results support the robustness of our conclusions. Notably, the induction of root-knot disease suppressiveness was accompanied by alterations in overall nematode community structure and an increased relative abundance in FLNs (especially Fu and OP groups) during continuous cropping. The positive effects of FLNs stem from bottom-up regulation, such as predation of specific bacterial and fungal taxa, and direct consumption of PPNs by OP nematodes[3,22]. While we did not collect fruit yield data, it is important to note that the observed suppression of root-knot nematodes and enrichment of free-living nematodes are generally associated with improved plant health and resilience[3,22]. Given that banana yield in long-term monoculture is strongly influenced by crop-intrinsic biological constraints, our results highlight nematode community shifts as an ecologically meaningful proxy for plant health outcomes in this system. Healthy plants generally exhibit higher nematode diversity than those infected with PPNs[22,28], suggesting that enrichment of certain FLN groups may be associated with reduced *Meloidogyne* prevalence. These results should be interpreted as correlative because we did not directly test their role in nematode suppression or plant growth

https://doi.org/10.1038/s41467-026-69647-y

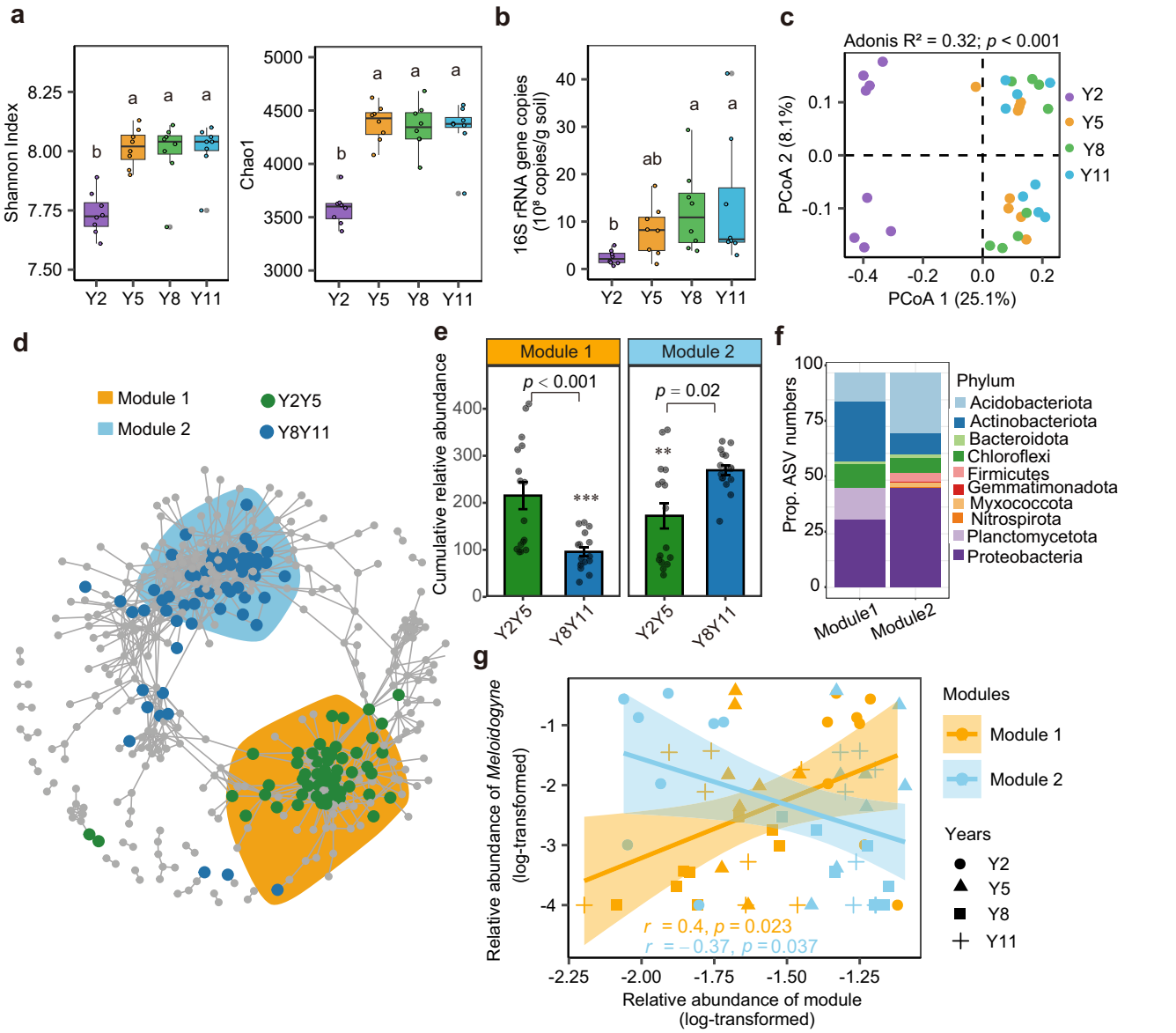

Fig. 4 | Long-term continuous cropping impacts bacterial communities and enriches special bacterial groups to suppress root-knot nematodes. a The Shannon index and Chao1 result reflect bacterial diversity changes. **b** Bacterial density in banana orchards cultivated continuously for 2 years (Y2), 5 years (Y5), 8 years (Y8), and 11 years (Y11). **c** The Principal coordinate analysis (PCoA) plot displays bacterial community composition based on the Bray-Curtis distances. **d** A meta co-occurrence network visualizing significant correlations between bacterial ASVs in the rhizosphere soil (Spearman's $\rho > 0.6$, $p < 0.01$, indicated with gray lines). This network comprised 32 samples, including two cropping times (Y2Y5, including samples from Y2 and Y5; Y8Y11, including samples from Y8 and Y11), with 16 replicates for each cropping time. Indicator ASVs are colored based on their association with different cropping times, and shaded areas represent network modules containing indicator ASVs. **e** Cumulative relative abundance of all ASVs from indicator modules in the network. The cumulative relative abundance indicates the overall response of indicator modules to different cropping times. (**f**) The taxonomic composition of indicator modules, shown as proportional ASVs numbers per phylum of bacteria. (**g**) Pearson correlation analysis between the relative abundance of the indicator modules and *Meloidogyne*. Shading associated with lines in the panel indicates a 95% confidence interval. For (**a**) and (**b**), boxplot center lines show the median, boxplot bounds show the first quartile Q1 and the third quartile Q3, and whiskers show 1.5 (Q3-Q1) below and above Q1 and Q3, black dots represent outliers and open dots represent individual values ($n = 8$ biologically independent samples), respectively. Statistical differences in (**a**) and (**b**) are indicated by distinct lowercase letters ($p \leq 0.05$) following the LSD test subsequent to one-way ANOVA. Multiple testing corrections are performed by BH algorithm. Two-sided tests were used for alternative hypothesis testing. For (**e**), values are means ± SD (n = 16 biologically independent samples). Asterisks indicate significant differences between the treatments based on two-sided tests by Student's *t*-test (*, $p < 0.05$; **, $p < 0.01$; ***, $p < 0.001$). Source data are provided as a Source Data file.

promotion. Therefore, future studies employing controlled inoculation of FLNs, both alone and in combination with microbial antagonists such as *Bacillus*, will be necessary to dissect their functional contributions to disease suppressiveness.

Beyond nematodes, our findings suggest that rhizomicrobiome also play a key role in mediating root-knot nematode disease outcomes. While prior studies often report a decline in microbial diversity under continuous cropping[29,30], we observed a clear increase in bacterial diversity over time in banana rhizospheres. High diversity in the soil microbiome has been associated with reduced incidence of soil-borne diseases[13], a pattern that was also evident in our field data. While total bacterial density increased with cropping duration, our data suggest that suppression of *Meloidogyne* is more closely linked to shifts in microbial community composition, rather than bulk bacterial abundance. This is consistent with previous studies emphasizing the functional and taxonomic specificity of disease-suppressive taxa[31,32].

https://doi.org/10.1038/s41467-026-69647-y

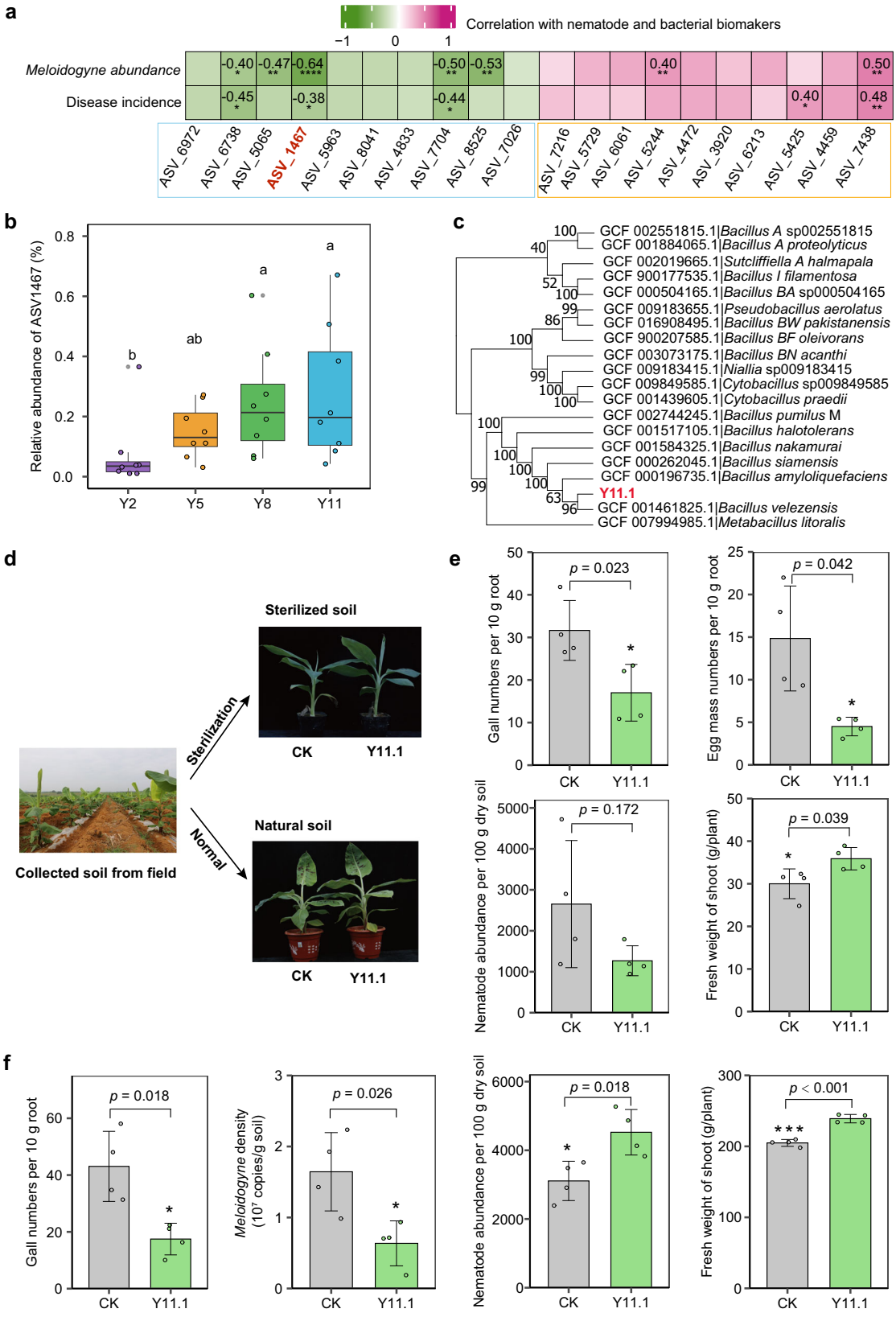

Moreover, we found that long-term continuous cropping of banana enriches specific bacterial taxa that associate with lower root-knot nematode disease incidence (Fig. 4). Given that plants are known to actively recruit beneficial microbes to the rhizosphere as part of their defense strategy[26,33,34], the elevated bacterial richness and enrichment of specific protective taxa in long-term banana fields likely contributes to the establishment of a disease-suppressive soil microbiome. Finally, while we focused on bacteria, other members of the microbiota might also be involved in nematode suppressiveness. Understanding the effects of such multi-kingdom interactions across different cropping time and geographical scales for nematode suppression will be the challenge of the future work.

Fig. 5 | Rhizobacteria ASV1467 was an essential taxon in root-knot nematode suppression. a The correlation between nematode data and the bacterial biomarkers identified by two complementary approaches (indicator species analysis and likelihood ratio tests). The table shows Spearman ρ correlations between the relative abundances of the top 10 indicator ASVs and *Meloidogyne* abundance, and disease incidence, indicated as heatmap spanning the continuum from negative (green) to positive (pink) correlations. Asterisks indicate the significant correlations (*, $p < 0.05$; **, $p < 0.01$; ***, $p < 0.001$, ****, $p < 0.0001$). **b** Relative abundance of ASV1467 in various continuous cropping times of banana. **c** Phylogenetic association of the isolate *Bacillus* Y11.1 with other complete sequences of strains from the literature based on 30 housekeeping genes as phylogenetic markers, using the neighbor-joining method with Molecular Evolutionary Genetics Analysis version 11. **d** Phenotypes of banana plants grown in sterilized and natural soil in greenhouse. **e** Gall and egg masses numbers, *Meloidogyne* abundance and the fresh weight of banana shoot in sterilized soil. **f** Gall numbers, *Meloidogyne* density and total nematode abundance in the soil, and the fresh weight of banana shoot in natural soil. For (**b**), boxplot center lines show the median, boxplot bounds show the first quartile Q1 and the third quartile Q3, and whiskers show 1.5 (Q3-Q1) below and above Q1 and Q3, and black dots represent outliers and open dots represent individual values ($n = 8$ biological replicates), Statistical differences in (**e**) and (**f**) are indicated by distinct lowercase letters ($p \leq 0.05$) following the LSD test subsequent to one-way ANOVA. Multiple testing corrections are performed by BH algorithm. Two-sided tests were used for alternative hypothesis testing. For (**e**) and (**f**), values are means ± SD (n = 4 biological replicates). Asterisks indicate significant differences between the treatments based on two-sided tests by Student's *t*-test (*, $p < 0.05$; **, $p < 0.01$; ***, $p < 0.001$). Source data are provided as a Source Data file.

Among the enriched taxa, *Bacillus* emerged as a keystone genus implicated in nematode suppression. We identified *B. velezensis* Y11.1 (ASV1467) as a taxon strongly associated with the field soils in a nematode suppressive state (Y8 and Y11). Functional assays confirmed its nematicidal activity, including the ability to kill *M. incognita* juveniles and significantly reduce root galling and nematode reproduction in both sterilized and natural soil systems (Fig. 5 and Supplementary Fig. 5). In this study, *B. velezensis* Y11.1 was applied weekly at high density to provide proof of concept for its suppressive activity against RKNs. While this approach is common in experimental biocontrol studies[35,36], we acknowledge that repeated applications are not realistic for field practice. Future field trials will therefore focus on testing single or reduced-frequency applications, and on determining the ecological conditions that allow *Bacillus* populations to persist and confer suppression more sustainably. The role of *Bacillus* spp. in biocontrol of root-knot nematodes is well-established and includes mechanisms such as toxin secretion, disruption of nematode attraction, and induction of systemic resistance in plants[37,38]. Several commercially-available *Bacillus* inoculants (e.g., *B. thuringiensis*, *B. subtilis*, and *B. cereus*) have been applied in agricultural production[16,17]. Our work adds an important dimension by showing that *B. velezensis* Y11.1 suppresses *M. incognita* through the production of the siderophore bacillibactin, which both kills and repels *Meloidogyne* in a concentration-dependent manner. Previous studies have shown that bacterial siderophores can suppress phytopathogens by sequestering iron, thereby depriving competitors of this essential nutrient[39,40]. Certain siderophores can also directly affect nematodes. For example, bacterial siderophores can induce mortality (pyoverdine produced by *Pseudomonas syringae*) in *C. elegans* or affect its development (enterobactin produced by *Escherichia coli*) and chemotaxis (pyoverdine secreted by *Pseudomonas aeruginosa*)[25,41,42]. Yet, little is known about bacterial siderophore effects on PPNs. Our results show that bacillibactin produced by *B. velezensis* Y11.1 repels and kills *M. incognita* (representatives PPNs,) but has no lethal effects on *C. elegans* (representative FLNs). In fact, bacillibactin was attractive to *C. elegans*, suggesting a potential dual function—suppressing PPNs while promoting FLNs recruitment and possibly proliferation. This conclusion is based on single species and future studies need to include a wider range of PPNs and FLNs. Previous studies demonstrated that certain bacterial siderophores promote the growth of *C. elegans* and serve as cues for locating bacterial prey, thereby expanding their population[41,42]. Taken together, our findings indicate that bacillibactin may contribute to the selective suppression of parasitic nematodes while favoring free-living nematodes in banana rhizospheres during long-term monoculture. While our results demonstrate that bacillibactin produced by *B. velezensis* Y11.1 can repel and reduce the viability of *Meloidogyne* spp., it is unlikely to be the sole suppressive factor. The genome of Y11.1 harbors multiple biosynthetic gene clusters, including those for lipopeptides (surfactin, fengycin, and iturin) and polyketides, which have been implicated in nematode antagonism[17]. The comparatively modest direct mortality caused by purified bacillibactin relative to the live strain suggests that other metabolites or synergistic effects may enhance the suppressive activity of Y11.1. Future work, including targeted mutagenesis and metabolite profiling, will be required to determine the relative contributions of these compounds to in situ nematode suppression. While our results reveal consistent spatiotemporal patterns in the abundance of FLNs and siderophore-producing *Bacillus*, we acknowledge that the observed relationships are correlative. Future studies using controlled co-inoculation systems will be essential to validate whether these organisms act synergistically or independently in promoting suppressiveness.

In conclusion, we demonstrated that long-term continuous cultivation of banana leads to an increase in FLNs and beneficial *Bacillus* spp. in the rhizosphere, fostering a disease-suppressive soil environment. We identified *B. velezensis* Y11.1 as a key agent in suppressing root-knot nematode infestation, in part through the secretion of bacillibactin—a siderophore that repels and kills *Meloidogyne* while attracting *C. elegans*, a model nematode for FLNs (Fig. 7). While our study focused on root-knot nematode suppressiveness, similar ecological principles may also apply to other important banana pathogens, such as *Fusarium* wilt. Exploring the interactions between nematodes, fungi, and rhizosphere microbes will be an important avenue for future research. Our evidence of PPNs biological control offers promising avenues for sustainable, nematicide-free disease management and supports the design of resilient cropping systems that promote both productivity and plant health.

Methods

Description of experimental site and sampling procedure

The study was conducted in a banana cultivation field located in Nanning, Guangxi, China (23°05´N, 107°82´E), characterized by a subtropical climate with an average annual temperature of 21.8 °C and mean annual precipitation of 1301 mm. The soil type in this area is a highly weathered Udic Ferralsol.

The field experiment spanned from March 2016 to October 2017, focusing on banana plants of the *Musa* AAA *Cavendish* cv. Williams B6 variety (Fig. 1a). Cultivation practice, including fertilization, and agronomic management remained consistent across the different time series plantations. Samples were collected using a space-for-time substitution approach. In 2016, we sampled four groups of banana plantations that had been continuously cropped for 1 (Y1), 4 (Y4), 7 (Y7), and 10 (Y10) years. In 2017, we re-sampled these same four groups of plantations, which by then had reached 2 (Y2), 5 (Y5), 8 (Y8), and 11 (Y11) years of continuous cropping (Fig. 1a). This design was chosen due to logistical constraints of banana constant growth and large in size that prevented sampling every cropping duration in both years, but it allowed us to represent the full temporal sequence of continuous cropping across sites. For each cropping duration (e.g., 1, 4, 7, or 10 years), 10 plantations (ranging from 1 to 2 ha) were randomly selected, and composite samples were obtained from five uniformly growing banana plants (200 g soil sample and 50 g root sample) using a five-point method. These 10

https://doi.org/10.1038/s41467-026-69647-y

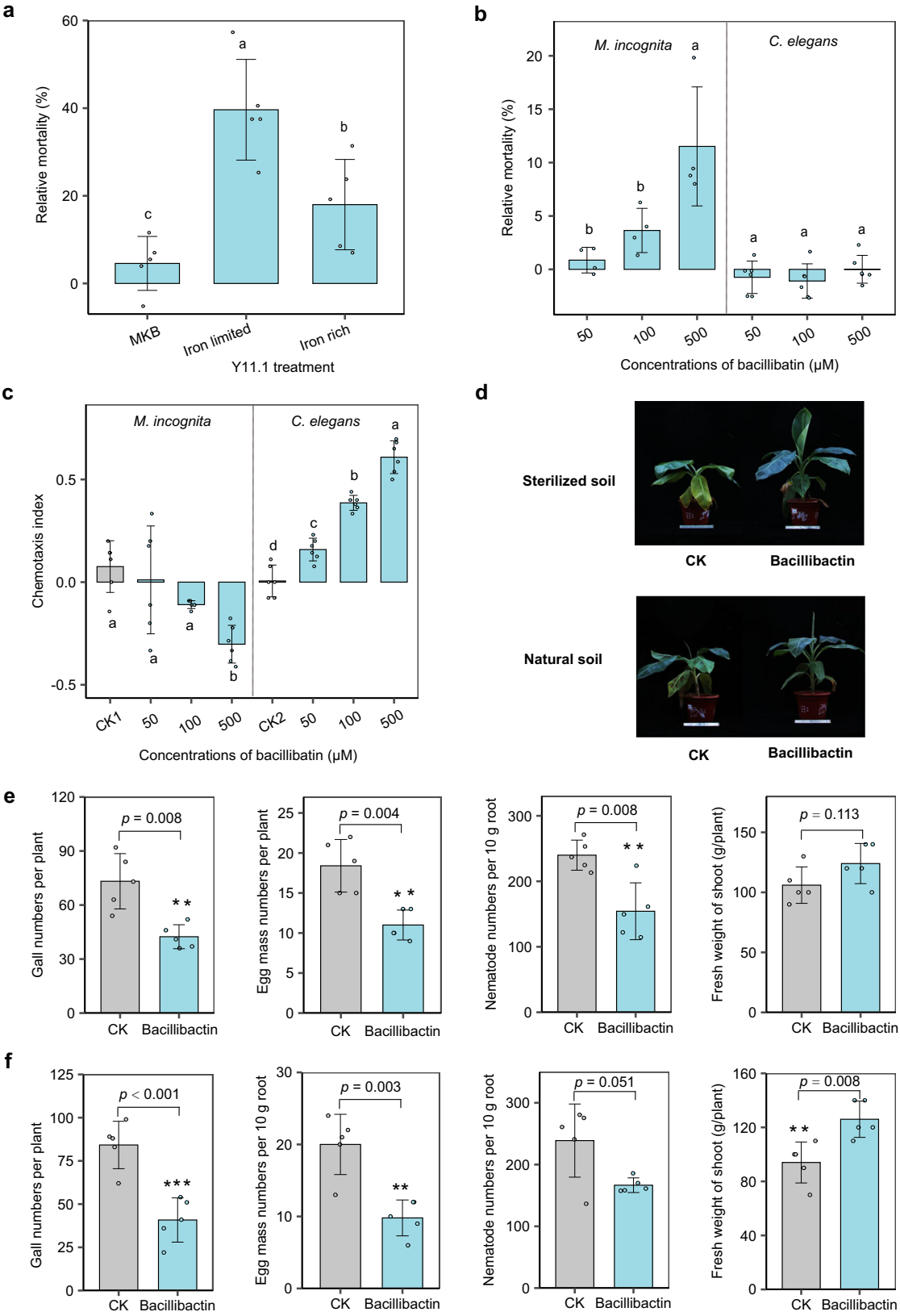

samples were treated as biological replicates for statistical analysis within each site. Sampling was conducted at three time points each year (March, July, and October) to capture seasonal variation in nematode infectivity and rhizosphere dynamics. Each field in 2016 was re-sampled in 2017 (e.g., Y1/Y2, Y4/Y5), ensuring consistency in spatial location across years. Initial analyses revealed no consistent differences across seasons or years, and therefore disease indices were averaged across seasons for each cropping year to reduce complexity and improve clarity in data presentation. Due to logistical constraints, we were unable to sample multiple independent plantations per cropping duration. Thus, this design uses a space-for-time substitution approach and reflects within-site variation.

Fig. 6 | Effect of bacillibactin on root-knot nematode suppression. a The relative mortality rate on *Meloidogyne incognita* J2s ($n = 5$ biologically independent samples) under MKB medium, iron-limited supernatant (high siderophore concentration + other secreted metabolites), and iron-rich supernatant (low siderophore concentration + other secreted metabolites). **b** The relative mortality rate on J2s of *Meloidogyne incognita* ($n = 4$ biologically independent samples) and *Caenorhabditis elegans* ($n = 6$ biologically independent samples) under various concentrations of bacillibactin. **c** The chemotaxis effects on J2s of *Meloidogyne incognita* ($n = 6$ biologically independent samples) and *Caenorhabditis elegans* ($n = 6$ biologically independent samples) under various concentrations of bacillibactin. **d** Phenotypes of banana plants grown in sterilized and natural soil in greenhouse. Gall and egg masses numbers, *Meloidogyne* abundance and the fresh weight of banana shoot in sterilized soil (**e**) and in natural soil (**f**). For (**a**–**c**), data represent as mean ± SD. Statistical differences were indicated by distinct lowercase letters ($p \le 0.05$) following the LSD test subsequent to one-way ANOVA. Multiple testing corrections are performed by BH algorithm. Two-sided tests were used for alternative hypothesis testing. For (**e**) and (**f**), Values are means ± SD ($n = 5$ biological replicates). Asterisks indicate significant differences between the treatments based on two-sided tests by Student's *t*-test (*, $p < 0.05$; **, $p < 0.01$; ***, $p < 0.001$). CK1, sterile water; CK2, M9 medium. Source data are provided as a Source Data file.

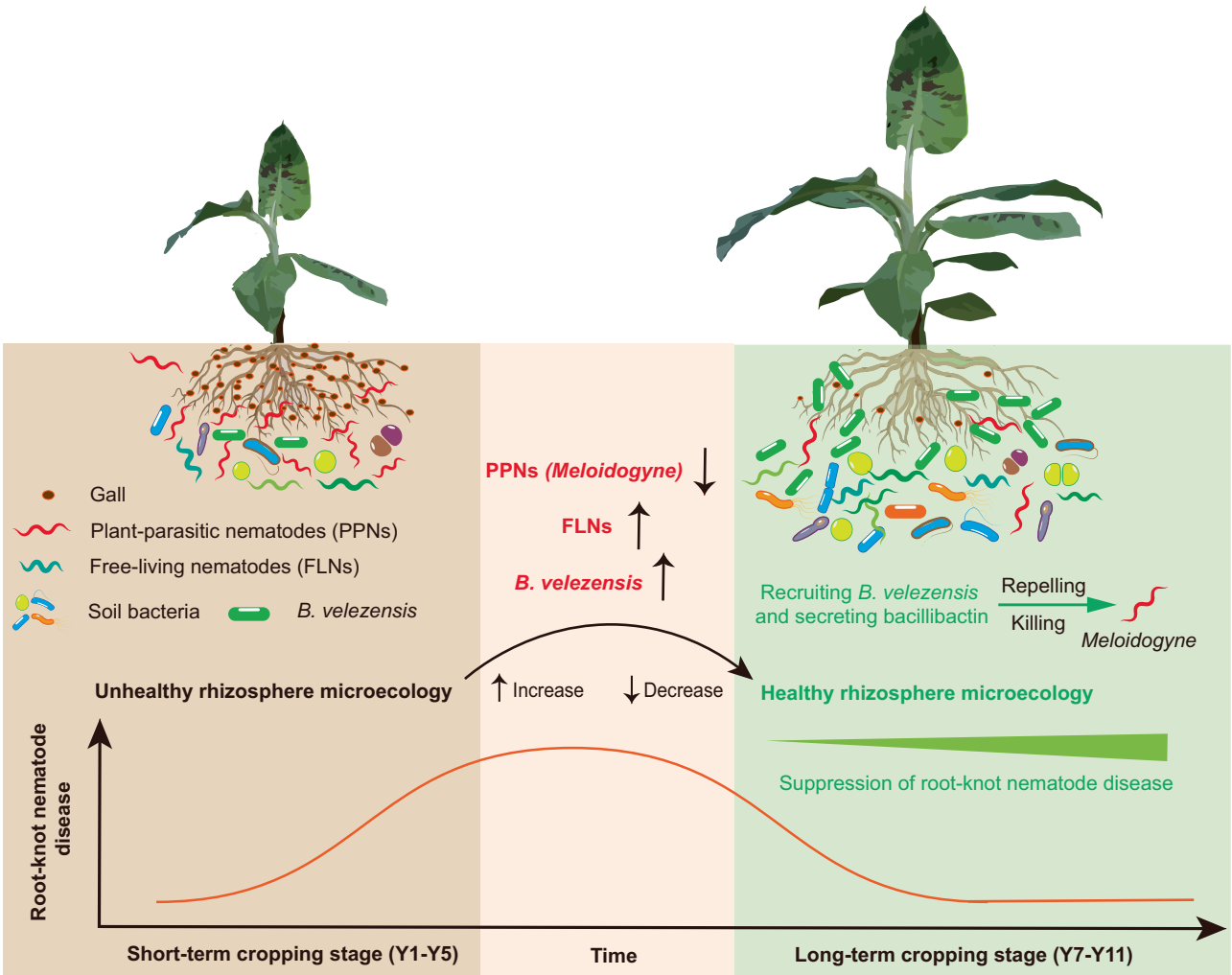

Fig. 7 | The mechanism underlying soil suppressiveness to root-knot nematode in long-term banana monoculture. The diagram illustrates the ecological transition in the banana rhizosphere from a disease-conducive to a disease-suppressive state across an 11-year continuous cropping system. During the short-term cropping stage (Years 1–5), the rhizosphere is characterized by low microbial diversity, enrichment of plant-parasitic nematodes (*Meloidogyne* spp., PPNs), and high disease incidence, indicated by root galls. Over time, rhizosphere microecology shifts with increasing abundance of free-living nematodes (FLNs), enrichment of *Bacillus velezensis*, and elevated microbial diversity. In the long-term stage (Years 7–11), *B. velezensis* secretes the siderophore bacillibactin, which repels and kills *Meloidogyne* while attracting FLNs, thereby reinforcing a healthy rhizosphere microbiome.

The root samples were collected per banana plant (50 g) for gall assessment. Galling of root systems was rated using a 0–5 rating scale[43]. The gall rate was assigned as: 0 = 0%, 1 = 1–15%, 2 = 15–30%, 3 = 30–50%, 4 = 50–75%, and 5 = 75–100% root galled, gall index = (gall rate × plant numbers)/(the highest gall rate × all plant numbers) × 100. For the Y1 field, where banana seedlings were planted in August 2016, the first sampling took place in October. Upon collection, soil samples were mixed thoroughly and sieved through a 2-mm sieve. The rhizosphere soil samples were stored at -80 °C for further analysis.

Analysis of soil nematode diversity

The soil nematodes were extracted from 100 g of soil using the modified Baermann funnel method and counted under a stereomicroscope[44]. After counting the soil nematode abundance, we identified nematodes (in 2016) further assigned into genus and four trophic groups, as bacterivores (Ba), fungivores (Fu), herbivores (He; Plant-parasitic, Pp), omnivores-predators (OP)[45]. A total of 60 nematode genera were identified, including 20 Ba, 13 Pp, 6 Fu, and 21 OP (Supplementary Tables 2-4). All of the soil nematodes were determined as colonizer–persister groups (cp1-5)[46]. Alpha diversity of the

nematode community was determined by the Shannon-Wiener diversity index (Shannon index), which was calculated as following: Shannon index =-∑Pi × ln Pi, in which 'Pi' represents the proportion of individuals of the 'i' group in the community.

In 2016 (Y1, Y4, Y7, Y10), nematode communities were assessed by morphological identification, which provides accurate relative abundances but is limited in throughput. In 2017 (Y2, Y5, Y8, Y11), high-throughput sequencing was applied to analyze nematode communities and, in parallel, rhizosphere microbial communities from the same soils. This sequential design was chosen to build on the first year's observations and to enable integrated microbial–nematode analyses, while reflecting practical constraints on resources and field logistics.

Soil DNA extraction, *16S rRNA* gene and *18S rRNA* gene amplicon sequencing

16S rRNA gene and *18S rRNA* gene amplicon sequencing were performed to examine the impact of continuous cropping on rhizosphere bacterial and nematode compositions, respectively. Total DNA was isolated from 500 mg rhizosphere soil sample using the FastDNA® Spin Kit for Soil (MP Biomedicals, Solon, USA) according to the manufacturer's instructions. The hypervariable region V3-V4 of the bacterial *16S rRNA* gene was amplified with primers 338 F (5′-ACTCCTACGGGAGGCAGCAG-3′) and 806 R (5′-GGACTACHVGGGTWTCTAAT-3′) by an ABI GeneAmp® 9700 PCR thermocycler (Applied Biosystems, Foster City, USA). Illumina MiSeq PE300 platform (Illumina, San Diego, USA) was used to sequence by the Majorbio Bio-Pharm Technology Co. Ltd. (Shanghai, China). For *18S rRNA* gene sequencing of soil nematodes, primers NF1F (5′-GGTGGTGCATGGCCGTTCTTAGTT-3′)[47] and NR (5′AGCGACGGGCGGTGTGTACAAA-3′)[48] were used. 18S rRNA primers were selected to specifically target soil nematodes, and therefore fungal taxa were underrepresented in the amplicon dataset. The amplification and sequencing were performed as described above.

The preprocessing of amplicon sequence data was conducted using usearch11.0.667. Following the removal of PCR primers and low-quality sequences, the bacterial community samples yielded 25519-40718 reads per group, while the soil eukaryote community samples ranged from 17852 to 48698 reads (275-19389 reads were taxonomically assigned to nematozoa per group). The processed reads were denoised and merged to generate amplicon sequence variants (ASVs). ASVs were taxonomically classified using the SINTAX algorithm in vsearch-2.23.0 and the SILVA release 138 database, with the exclusion of mitochondrial and chloroplast reads. Additionally, features with a total abundance of less than three across all samples were filtered out. This process resulted in 8725 bacterial features (Supplementary Data 2) derived from the 16S rRNA V3-V4 region and 149 nematode features (Supplementary Data 3) from the 18S rRNA V4 region. 16.5% of the 18S rRNA reads were identified to 29 nematode taxa (Supplementary Data 4 and Supplementary Table 5).

Quantitative PCR of rhizobacteria

Total bacterial abundance in the rhizosphere was quantified using quantitative PCR (qPCR) with primers 338 F/806 R for the assessment of total soil bacterial density. The total soil DNA was extracted as described above, and subsequent to DNA quantification and concentration assessment, the qPCR assays were performed according to the standard protocols by Majorbio Bio-Pharm Technology Co. Ltd. (Shanghai, China). Briefly, the PCR reaction mixture (20 μL) contained 10 μL ChamQ SYBR Color qPCR Master Mix (2X), 0.4 μL each primer (5 μM), 2 μL template DNA (10 ng/μL) and 7.2 μL ddH_2O, with each DNA sample analyzed in three replicates. Following confirmation of the amplified fragment's specificity by melt analysis and agarose gel electrophoresis. The thermal cycling profile include a first step at 95 °C for 5 min, followed by 40 cycles of 95 °C for 30 s and 56 °C for 30 s, with a final extension at 72 °C for 40 s, and extension at 72 °C for 10 min. The results were expressed as copies/g soil by calculating the copy number of the target fragment from the standard.

Isolation and identification of rhizobacteria

Rhizobacteria were isolated from the rhizosphere of Y8 and Y11, where the disease index decreased (Fig. 1b). Briefly, one gram of the soil samples was agitated in 9 mL sterilized deionized water for 10 min. The resulting microbial suspension was serially diluted tenfold and spread onto Luria-Bertani (LB) agar plates. Incubation was carried out at 30 °C for 48 h in darkness. Colonies with distinct morphologies were selected and re-streaked on LB plates for further purification. The final collection consisted of 190 rhizobacteria isolates. Purified isolates were cultured in liquid LB medium at 30 °C with shaking at 180 r.p.m. The *16S rRNA* gene of the rhizobacterial isolates was amplified using 27 F (5′-AGAGTTTGATCMTGGCTCAG-3′) and 1492 R (5′-TACGGYTACCTTGTTACGACTT-3′) to generate phylogenetic information. The crude electropherograms were analyzed by the MEGAv.11.0 software. The isolated strains sequences were compared with other sequences using the BLAST in the NCBI database followed by phylogenetic analysis with the neighbor-joining (NJ) method in the MEGA software. Y11.1 sequence was deposited at GenBank, and the accession numbers was PP789636.

Total genomic DNA extraction and identification of *Bacillus* Y11.1

The genome of *Bacillus* Y11.1 isolate was sequenced using a combination of PacBio RS II Single Molecule Real Time (SMRT) and Illumina sequencing platforms. *Bacillus* Y11.1 and 19 other strains with complete genome sequences were selected to construct a phylogenetic tree with 30 housekeeping genes as phylogenetic markers, and employed the NJ method with MEGAv.11.0. All analyses were performed on the I-Sanger Cloud Platform from Shanghai Majorbio. The genome mining for biosynthetic gene clusters of antimicrobial compounds was conducted with antiSMASH 7.0[49]. Siderophore biosynthesis was further investigated with detailed blast and literature comparisons.

Assessing the nematicidal activity of *B. velezensis* Y11.1

To assess the nematicidal activity of *B. velezensis* Y11.1, we conducted in vitro experiments using LB medium. Cultures were grown at 30 °C with shaking at 180 r.p.m until reaching OD_{600} = 1.0. After filtering through a 0.22 μm membrane, the culture was diluted with LB medium to concentrations of 1x, 0.5x, and 0.1x. All solutions were supplemented with 100 μg/mL rifampicin, 20 μg/mL penicillin, and 50 μg/mL streptomycin to avoid contamination. A total of approximately 100 *M. incognita* J2s in a 10 μL suspension and 500 μL of different dilutions of LB culture medium were added into 24-well culture plates, with distilled water (CK1) and LB medium (CK2) used as controls. After incubation for 48 hrs at 28 °C, 20 μL of 1 M NaOH solution was added before quantification live and dead J2s. Nematodes exhibiting body movement were categorized as alive, while those unresponsive were considered dead[50]. Each treatment was replicated six times, and the mortality of J2s was calculated as following: Relative mortality = (treatment mortality/control mortality)/(100-control mortality) ×100%.

Pot experiment of *B. velezensis* Y11.1

Two pot experiments, using normal and sterilized soil, were conducted in the greenhouse (China Agricultural University, Beijing, China, coordinates: 40°1′N, 116°16′E; 30/22 °C and a 14/10 hrs light/dark cycle at 60-70% humidity) from June to September 2022. Soil from a banana field in Nanning, Guangxi, China was characterized by a pH of 4.42 (in 1 mol/L KCl), and concentrations of organic matter, N, Olsen-P, and NH_4OAc-K at 28.39 g/kg, 29.04 mg/kg, 3.78 mg/kg, and 117.27 mg/kg, respectively. Banana seedlings (*Musa* AAA *Cavendish* cv. Williams B6) were initially grown in vermiculite for 45 days before transplanting. For

soil sterilization treatment, the soil was γ-irradiated (^{60}Co-γ) with a maximum dose of 20 kGy for 24 h (Beijing Atomic High-tech Jinhui Radiation Technology Application Co. Ltd.). Seedlings were transplanted into 10 cm diameter plastic pots containing 0.5 kg of radiation-sterilized red soil. 50 mL of *B. velezensis* Y11.1 solution (10^6 CFU mL^{-1}) were irrigated into the rhizosphere every 7 days, with 50 mL of water used as control. A total of 1000 *Meloidogyne incognita* second-stage juveniles (J2s, incubated at 28 °C within 3 days) were inoculated after the initial solution application, and plant and soil samples were collected 35 days post-inoculation. For normal soil treatment, seedlings were transplanted into 3 kg natural soil in 20 cm diameter plastic pots. Seven days post-transplantation, 300 mL of *B. velezensis* Y11.1 solution (10^6 CFU mL^{-1}) were irrigated into the rhizosphere, with 3000 *Meloidogyne incognita* J2s inoculated simultaneously. *B. velezensis* Y11.1 solution was applied every 7 days, and 300 mL of water served as a control. Banana plants were harvested 60 days after J2s inoculation, and after measuring plant biomass, roots were carefully washed, and galls and egg masses from 10 g root sample were quantified. Soil nematodes were extracted and counted and then stored at -80 °C for root-knot nematode analysis. Each treatment consisted of four replicates.

Quantitative PCR of root-knot nematode

Soil nematode DNA from pot experiments under natural soil condition was extracted. The quality and concentration of DNA were assessed by 1.0% agarose gel electrophoresis and the NanoDrop® ND-2000 spectrophotometer (Thermo Scientific Inc., USA). The hypervariable region D2/D3 of the nematode 28S rDNA gene were amplified with root-knot nematode species-specific primer pairs RK28SF: 5′-CGGATAGAGTCGGCGTATC-3′ and MR: 5′-AACCGCTTCGGACTTCCACCAG-3′ with an ABI GeneAmp 7300 PCR thermocycler (ABI, CA, USA)[51]. The PCR reaction mixture consisted 4 μL 2x ChamQ SYBR Color qPCR Master Mix, 0.4 μL each primer (5 μM), 0.2 μL 50 x ROX Reference Dye 1, 1 ng template DNA, and ddH_2O to a final volume of 10 μL. The PCR amplification cycling conditions included an initial denaturation at 95 °C for 3 min, followed by 40 cycles of denaturing at 95 °C for 5 s, annealing at 58 °C for 30 s, and extension at 72 °C for 1 min, and with a final step at 4 °C. All samples were amplified in triplicate, and the specificity of the amplified fragments was confirmed by analyzing melt curves and electrophoresis on agarose gels. The results were expressed as copies/g soil by calculating the copy number of the target fragment from the standard curves.

Purification and quantitative assessment of bacillibactin production in *B. velezensis* Y11.1

Bacillibactin production by *B. velezensis* Y11.1 was assessed in iron-depleted liquid standard succinic medium (SSM) without additional iron (6 g L^{-1} K_2HPO_4, 3 g L^{-1} KH_2PO_4, 1 g L^{-1} $(NH_4)_2SO_4$, 0.2 g L^{-1} $MgSO_4{\cdot}7H_2O$, 4 g L^{-1} succinic acid, pH = 7.0) (Fig. 1c). After 48 hrs of incubation at 30 °C, cultures were diluted to OD_{600} = 0.8. Supernatant were collected following centrifugation (9400 g, 10 min at 4 °C) and filtration (using a 0.22 μm filter). Bacillibactin concentration was determined using a modified version of the chrome azurol S (CAS) assay[52]. Briefly, 4.3079 g of anhydrous piperazine was dissolved in 30 mL of water and adjusted the pH to 5.6 with HCl. Subsequently, 21.9 mg of HDTMA was dissolved in 50 mL water. Concurrently, a solution was prepared by mixing 1.5 mL of 1 mM $FeCl_3{\cdot}6H_2O$ (in 10 mM HC1) with 7.5 mL of 2 mM CAS. This solution was added to the HDTMA solution, and the mixture volume was adjusted to 100 mL with deionized water. One milliliter of supernatant was combined with an equal volume of CAS solution in a 2-mL centrifuge tube; deionized water served as a control. After 4 hrs of incubation at room temperature, after diluting the supernatants towfold, the OD_{630} of the supernatants (As) and deionized water (Ar) was measured by a plate reader (SpectraMax M5, Molecular Devices, Sunnyvale, USA). Bacillibactin-secreting capacity was quantified as Su = (Ar-As)/Ar. A calibration curve was established using desferrioxamine B (DFOB) to estimate bacillibactin concentration in *B. velezensis* Y11.1 supernatant (calibration curve equation: bacillibactin equivalent μM = (32.99 × Su + 0.2746) × 2, R^2 = 0.999, $p < 0.001$).

The production and purification of bacillibactin were conducted following established protocol[52]. Briefly, *B. velezensis* Y11.1 was cultured in 10 L SSM medium at 30 °C and 180 r.p.m for 48 h. The culture media was centrifuged at 12000 g for 15 min and the resulting supernatant was filtrated. The culture medium was adjusted to pH 5.5 (using HCl) and adsorbed by XAD-4 resin. The bacillibactin-containing fraction was eluted using MeOH-H_2O (1:1, v/v). The eluate was evaporated to dryness under vacuum. To enhance purity, the collected dry matter was subjected to a second adsorption by XAD-4 and elution with MeOD-H_2O (1:1, v/v). The second eluate was concentrated to 5 mL, passed through a dextran gel (LH-20) column using MeOH-H_2O 1:1 (v/v) as eluent to obtain the purified bacillibactin-containing fraction, which was then evaporated to dryness under vacuum.

Assessing the nematicidal activity of siderophore bacillibactin

To verify whether siderophore bacillibactin production affects nematode mortality, we cultured *B. velezensis* Y11.1 in iron-limited and iron-rich conditions. MKB medium (2.5 g l^{-1} K_2HPO_4, 2.5 g l^{-1} $MgSO_4{\cdot}7H_2O$, 15 ml l^{-1} glycerin and 5.0 g l^{-1} casamino acids, pH 7.2) contains low quantities of residual iron but still allows *B. velezensis* Y11.1 to grow to a certain extent regardless of their ability to produce siderophores (iron-limited condition). As an iron-rich medium, the MKB medium was added with 50 μM $FeCl_3$. Cultures were grown at 30 °C with shaking at 180 r.p.m 48 hrs. After centrifugation (4400 g, 5 min at 4 °C) and filtration (through 0.22 μm membrane), the cell-free supernatants were used to assayed the lethal effects of *Meloidogyne* J2s. MKB medium (used as control), iron-limited supernatant, and iron-rich supernatant were tested. a total of approximately 800 *M. incognita* J2s in a 1 mL suspension and 1 mL different supernatants were added into 24-well culture plates. After 48 hrs at 28 °C, 20 μL of 1 M NaOH solution was added before quantification live and dead J2s. The mortality rate was calculated as described above.

We next investigated the lethal test using purified bacillibactin on *M. incognita* and *C. elegans*. (1) The *Meloidogyne* juveniles (J2s) were incubated sterile water, dissolving the purified bacillibactin in sterile water to 100, 200, and 1000 μM. A volume of 500 μL *Meloidogyne* juveniles (containing approximately 100 J2s) and 500 μL various concentrations of bacillibactin were pipetted into 24-well cell culture plates. A volume of 1 mL sterile water was used as a control. The plates were then incubated at 25 °C for 48 hrs. Counting the dead nematodes as described above. (2) Age-synchronized *C. elegans* juveniles (18 hrs) were cultured in M9 medium (3 g/L KH_2PO_4, 6 g/L Na_2HPO_4, 5 g/L NaCl, 1 mL 1 M $MgSO_4$) to a density of 100 juveniles per 500 μL. The purified bacillibactin were dissolved in M9 medium to 100, 200, and 1000 μM. A volume of 500 μL various concentrations of bacillibactin solutions and 500 μL *C. elegans* age-synchronized culture medium (containing approximately 100 J2s) were added into 24-well cell culture plates. M9 medium served as control. After incubating at 20 °C for 48 hrs, the dead nematodes were counted as described above.

Chemotaxis assay of bacillibactin with *M. incognita* and *C. elegans*

Chemotaxis assays were conducted to investigate the effects on the chemotactic motility of *M. incognita* and *C. elegans* under SSM medium and purified bacillibactin. Two lines were drawn 0.5 cm from the center at the bottom of 9 cm Petri dishes, and two points were drawn 1.0 cm from the lines and 1.5 cm from the center. A volume of 10 mL of 1% agar was added to petri dishes and allowed to dry. (1) For the chemotaxis assays of *B. velezensis* Y11.1 cultured in SSM medium on *M. incognita*, supernatant obtained as described above was used. The supernatant

was diluted with SSM medium to concentrations of 0.01x, 0.1x, 0.5x, and 1x. Various concentrations of supernatant (50 μL) were placed on one point on the agar surface, while 50 μL of SSM medium was placed on the other point as a control. Approximately 100 *M. incognita* J2s (50 μL) were added to the center of the plate. After a 6-hour incubation at 28 °C, nematodes on the treated and control sides were counted. The chemotaxis index was calculated using the formula: chemotaxis index = (nematodes on the treated side - nematodes on the control side)/(nematodes on the treated side + nematodes on the control side). (2) For the chemotaxis assays of bacillibactin on *M. incognita*, the purified bacillibactin was diluted with sterile water to 50, 100, and 500 μM, 50 μL of various bacillibactin solutions were added to one point on the agar surface and 50 μL sterile water was added to other point, 50 μL *M. incognita* (approximately 100 J2s) was added on the center of the plate. Nematode were counted after a 6-hour incubation at 28 °C. (3) For the chemotaxis assays of bacillibactin on *C. elegans*, various concentrations of bacillibactin diluted with M9 medium (50, 100, and 500 μM) were tested. The next step of chemotaxis assays is described above. *C. elegans* were counted after a 6-hour incubation at 20 °C.

Pot experiment of bacillibactin

We identified the effect of bacillibactin in two pot experiments (normal and sterilized soil) from May to October 2024. The greenhouse, soil and banana seedlings were as described above. Seedlings were transplanted into 20 cm diameter plastic pots containing 3.0 kg of radiation-sterilized or natural red soil. A volume of 300 mL of bacillibactin solution (400 μM) were irrigated into the rhizosphere every 14 days, with 300 mL of water used as control. A total of 1800 *M. incognita* J2s were inoculated 7 days after the initial solution application. The plant and soil samples were collected 110 days post-inoculation. After measuring plant biomass, roots were carefully washed, and we counted the total galls and egg masses in the entire root system, and quantified the plant-parasitic nematodes abundance in 10 g root. Each treatment consisted of five replicates.

Statistical Analyses

Statistical analysis was conducted by using student *t*-test, two-way analysis of variance (ANOVA) with LSD as post-hoc test, as indicated in the Figure legends. A p-value < 0.05 was considered significant. The principal coordinate analysis (PCoA) and Bray-Curtis distance calculation were performed by R (v4.1.3) 'phyloseq' package (v.1.34.0). A co-occurrence network was constructed with all samples (two cropping times: Y2Y5, including samples from Y2 and Y5; Y8Y11, including samples from Y8 and Y11, each with 16 replicates). Our aim was to identify the ecological clusters of strongly associated ASVs, according to the methodology by Jiang et al. [53]. Indicator species analysis and likelihood ratio tests (LRTs) were employed pinpoint bacterial ASVs most significantly responsive to root-knot nematode suppression. Briefly, filtered communities were normalized using the BIOCONDUCTOR package EDGER, expressing normalized values as relative abundance counts per million (CPM)[54]. The R package INDICSPECIES was used to identify ASVs responsible for observed suppression effects through correlation-based indicator species analysis, with 10^4 permutations and significance set at $p < 0.05$. Differential ASV abundance between cropping times was tested using LRTs with R package EDGER, considering a false-discovery rate-adjusted value of $p < 0.05$ as indicative of responsiveness to cropping times. Indicator ASVs to cropping times were defined through both indicators species analysis and LRTs. Network modules, identified as substructures with a higher density of edges within groups than between them, were identified by calculating pairwise Spearman's rank correlations between ASVs and using R package IGRAPH. Positive and significant correlations (Spearman's $\rho > 0.6$, $p < 0.01$) and main modules in the network were visualized with the R package IGRAPH. Linear regression models were used to demonstrate the relationship between the relative abundance of the indicator modules and the relative abundance of *Meloidogyne* in the co-occurrence network. To identify the key microbial predictors of *Meloidogyne* abundance, Random Forest (RF) regression was performed using the R packages randomForest and rfPermute. Predictor variables consisted of the 40 most abundant ASVs from the two indicator modules (top 20 ASVs each from Module 1 and Module 2). The RF model was constructed using 500 regression trees (ntree = 500) with the importance = TRUE parameter enabled. The contribution of each ASV was quantified by the percentage increase in mean squared error (%IncMSE), and its statistical significance was determined through 1000 permutations (nrep = 1000). Plots including conceptual diagrams were assembled and aesthetically perfected by Adobe Illustrator CC, 2023 (Adobe, San Jose, USA).

Reporting summary

Further information on research design is available in the Nature Portfolio Reporting Summary linked to this article.

Data availability

The clean data of 16S rRNA and 18S rRNA amplicon sequencing used in this study are deposited in the NCBI database under accession code PRJNA1148900 and PRJNA1148914, respectively. The *16S rRNA* gene sequences of *B. velezensis* Y11.1 isolated rhizobacteria is deposited on GenBank with accession code PP789636. The *B. velezensis* Y11.1 reference strain genome sequence is available in the NCBI database under accession code PRJNA1110842. Source data are provided with this paper.

Code availability

The analysis code that supports the findings of this study is available on GitHub (https://github.com/91Lu/Soil-suppressive-of-banana-root-knot-nematode) and deposited in the Zenodo[55] (https://doi.org/10.5281/zenodo.18476452).

References

1. Delgado-Baquerizo, M. et al. The proportion of soil-borne pathogens increases with warming at the global scale. *Nat. Clim. Change* **10**, 550–554 (2020).
2. Savary, S. et al. The global burden of pathogens and pests on major food crops. *Nat. Ecol. Evol.* **3**, 430–439 (2019).
3. Topalović, O. & Geisen, S. Nematodes as suppressors and facilitators of plant performance. *New Phytol* **238**, 2305–2312 (2023).
4. Sikora, R. A. et al. Integrated nematode management in a world in transition: constraints, policy, processes, and technologies for the future. *Annu. Rev. Phytopathol.* **61**, 209–230 (2023).
5. Zhang, J. et al. Changes in the microbiome in the soil of an American ginseng continuous plantation. *Front. Plant. Sci.* **11**, 572199 (2020).
6. Hamid, M. I. et al. Successive soybean-monoculture cropping assembles rhizosphere microbial communities for the soil suppression of soybean cyst nematode. *FEMS Microbiol. Ecol.* **93**, fiw222, (2017).
7. Zhou, Y. et al. Crop rotation and native microbiome inoculation restore soil capacity to suppress a root disease. *Nat. Commun.* **14**, 8126 (2023).
8. Luquini, L., Barbosa, D., Haddad, F., Ferreira, C. F. & Amorim, E. P. Nematode survey and biochemical characterization of *Meloidogyne* spp. in a main banana production area in Brazil. *Crop Prot* **117**, 94–99 (2019).
9. Lu, Q. et al. Nematicidal effect of methyl palmitate and methyl stearate against *Meloidogyne incognita* in bananas. *J. Agric. Food Chem.* **68**, 6502–6510 (2020).
10. Su, L. et al. Isolation of antagonistic endophytes from banana roots against *Meloidogyne javanica* and their effects on soil nematode community. *Front. Microbiol.* **8**, 2070 (2017).

11. Raaijmakers, J. M. & Mazzola, M. Soil immune responses soil microbiomes may be harnessed for plant health. *Science* **352**, 1392–1393 (2016).
12. Costa, LSAS. et al. Repeated exposure of wheat to the fungal root pathogen *Bipolaris sorokiniana* modulates rhizosphere microbiome assembly and disease suppressiveness. *Environ. Microbiome* **18**, 85 (2023).
13. Schlatter, D., Kinkel, L., Thomashow, L., Weller, D. & Paulitz, T. Disease suppressive soils: new insights from the soil microbiome. *Phytopathology* **107**, 1284–1297 (2017).
14. Wen, T. et al. Deciphering the mechanism of fungal pathogen-induced disease-suppressive soil. *New Phytol* **238**, 2634–2650 (2023).
15. Topalović, O. & Heuer, H. Plant-nematode interactions assisted by microbes in the rhizosphere. *Curr. Issues. Mol. Biol.* **30**, 75–88 (2019).
16. Shi, J. & Sun, M. *Bacillus* thuringiensis: a gift for nematode management. *Trends Parasitol* **41**, 235–246 (2025).
17. Vasantha-Srinivasan, P., Park, K. B., Kim, K. Y., Jung, W. J. & Han, Y. S. The role of *Bacillus* species in the management of plant-parasitic nematodes. *Front. Microbiol.* **15**, 1510036 (2024).
18. Gine, A., Carrasquilla, M., Martinez-Alonso, M., Gaju, N. & Sorribas, F. J. Characterization of soil suppressiveness to root-knot nematodes in organic horticulture in plastic greenhouse. *Front. Plant Sci.* **7**, 164 (2016).
19. Westphal, A. Detection and description of soils with specific nematode suppressiveness. *J. Nematol.* **37**, 121–132 (2005).
20. Topalović, O. et al. Deciphering bacteria associated with a pre-parasitic stage of the root-knot nematode *Meloidogyne hapla* in nemato-suppressive and nemato-conducive soils. *Appl. Soil Ecol.* **172**, 104344 (2022).
21. Wilschut, R. A. & Geisen, S. Nematodes as drivers of plant performance in natural systems. *Trends Plant Sci* **26**, 237–247 (2021).
22. Li, G., Liu, T., Whalen, J. K. & Wei, Z. Nematodes: an overlooked tiny engineer of plant health. *Trends Plant Sci.* **29**, 52–63 (2023).
23. Tejeda-Benitez, L. & Olivero-Verbel, J. *Caenorhabditis elegans*, a biological model for research in toxicology. *Rev. Environ. Contam. Toxicol.* **237**, 1–35 (2016).
24. Kirienko, N. V. et al. *Pseudomonas aeruginosa* disrupts *Caenorhabditis elegans* iron homeostasis, causing a hypoxic response and death. *Cell Host Microbe* **13**, 406–416 (2013).
25. Bashir, A. et al. Pyoverdine-mediated killing of *Caenorhabditis elegans* by *Pseudomonas syringae* MB03 and the role of iron in its pathogenicity. *Int. J. Mol. Sci.* **21**, 2198 (2020).
26. Carrion, V. J. et al. Pathogen-induced activation of disease-suppressive functions in the endophytic root microbiome. *Science* **366**, 606–612 (2019).
27. Kim, D. R. et al. Function and distribution of a lantipeptide in strawberry *Fusarium* wilt disease–suppressive soils. *Mol. Plant-Microbe Interact.* **32**, 306–312 (2019).
28. Hoang, H. et al. Investigation of the soil nematode community composition in a monoculture Robusta coffee plantation in Dak Lak, Vietnam. *Glob. Ecol. Conserv.* **32**, e01932 (2021).
29. Pang, Z. et al. Soil metagenomics reveals effects of continuous sugarcane cropping on the structure and functional pathway of rhizospheric microbial community. *Front. Microbiol.* **12**, 627569 (2021).
30. Li, Y. et al. Effects of different continuous cropping years on bacterial community and diversity of cucumber rhizosphere soil in solar-greenhouse. *Curr. Microbiol.* **78**, 2380–2390 (2021).
31. Hussain M. et al. Redundancy in microbiota-mediated suppression of the soybean cyst nematode. *Microbiome* **12**, 125 (2024).
32. Shen, Z. et al. Shared core microbiome and functionality of key taxa suppressive to banana *Fusarium* wilt. *Research* **2022**, 9818073 (2022).
33. Mendes, R. et al. Deciphering the rhizosphere microbiome for disease-suppressive bacteria. *Science* **332**, 1097–1100 (2011).
34. Trivedi, P., Leach, J. E., Tringe, S. G., Sa, T. & Singh, B. K. Plant-microbiome interactions: from community assembly to plant health. *Nat. Rev. Microbiol.* **18**, 607–621 (2020).
35. Hansel, J., Saville, A. C. & Ristaino, J. B. Evaluation of a formulation of *Bacillus subtilis* for control of Phytophthora blight of bell pepper. *Plant Dis* **108**, 1014–1024 (2024).
36. Doherty, J. R. & Roberts, J. A. Topdressing biochar compost mixtures and biological control organism applications suppress foliar pathogens in creeping bentgrass fairway turf. *Plant Dis* **107**, 2346–2351 (2023).
37. Xun, W. et al. Sustained inhibition of maize seed-borne *Fusarium* using a *Bacillus*-dominated rhizospheric stable core microbiota with unique cooperative patterns. *Adv. Sci.* **10**, e2205215 (2023).
38. Ghahremani, Z. et al. *Bacillus firmus* Strain I-1582, a nematode antagonist by itself and through the plant. *Front. Plant Sci.* **11**, 796 (2020).
39. Saha, M. et al. Microbial siderophores and their potential applications: a review. *Environ. Sci. Pollut. Res.* **23**, 3984–3999 (2016).
40. Gu, S. et al. Competition for iron drives phytopathogen control by natural rhizosphere microbiomes. *Nat. Microbiol.* **5**, 1002–1010 (2020).
41. Hu, M., Ma, Y. & Chua, S. L. Bacterivorous nematodes decipher microbial iron siderophores as prey cue in predator-prey interactions. *Proc. Natl. Acad. Sci. U.S.A.* **121**, e2314077121 (2024).
42. Qi, B. & Han, M. Microbial siderophore enterobactin promotes mitochondrial iron uptake and development of the host via interaction with ATP synthase. *Cell* **175**, 571–582 (2018).
43. Bridge, J. & Page, S. L. J. Estimation of root-knot nematode infestation levels on roots using a rating chart. *Trop. Pest Management* **26**, 296–298 (1980).
44. Viglierchio, D. R. & Schmitt, R. V. On the methodology of nematode extraction from field samples: comparison of methods for soil extraction. *J. Nematol.* **15**, 450–454 (1983).
45. Yeates, G. W., Bongers, T., Goede, R. G. D., Freckman, D. W. & Georgieva, S. S. Feeding habits in soil nematode families and genera—an outline for soil ecologists. *J. Nematol.* **25**, 315–331 (1993).
46. Bongers, T. & Bongers, M. Functional diversity of nematodes. *Appl. Soil Ecol.* **10**, 239–251 (1998).
47. Porazinska, D. L. et al. Evaluating high-throughput sequencing as a method for metagenomic analysis of nematode diversity. *Mol. Ecol. Resour.* **9**, 1439–1450 (2009).
48. Darby, B. J., Todd, T. C. & Herman, M. A. High-throughput amplicon sequencing of rRNA genes requires a copy number correction to accurately reflect the effects of management practices on soil nematode community structure. *Mol. Ecol.* **22**, 5456–5471 (2013).
49. Blin, K. et al. antiSMASH 7.0: new and improved predictions for detection, regulation, chemical structures and visualisation. *Nucleic Acids Res.* **51**, W46–W50 (2023).
50. Fráguas, R. M. et al. Toxicities of 4,5-Dihydroisoxazoles against root-knot nematodes and in silico studies of their modes of action. *J. Agric. Food Chem.* **68**, 523–529 (2020).
51. Ye, W., Zeng, Y. & Kerns, J. Molecular characterisation and diagnosis of root-knot nematodes (*Meloidogyne* spp.) from Turfgrasses in North Carolina, USA. *PLoS One* **10**, e0143556 (2015).
52. Wang, N. et al. Microbiome convergence enables siderophore-secreting-rhizobacteria to improve iron nutrition and yield of peanut intercropped with maize. *Nat. Commun.* **15**, 839 (2024).
53. Jiang, Y. et al. Nematodes and their bacterial prey improve phosphorus acquisition by wheat. *New Phytol* **237**, 974–986 (2023).

54. Hartman, K. et al. Cropping practices manipulate abundance patterns of root and soil microbiome members paving the way to smart farming. *Microbiome* **6**, 14 (2018).
55. Lu, Q. et al. Siderophore-producing *Bacillus* and free-living nematodes mediate soil suppressiveness to banana root-knot nematodes. 91Lu/Soi-suppressive-of-banana-root-knot-nematode. *Zenodo*. https://doi.org/10.5281/zenodo.18476452 (2026).

Acknowledgements

This research was financially supported by the National Natural Science Foundation of China (grant no. 32372810 to Y.-M. Z., 32302668 to Q.-F. L., and 42577142 to S.-H. G.), and the National Key Research and Development Program of China (grant no. 2022YFD1901500/2022YFD1901501 and 2023YFD1700203 to Y.-M. Z.), the Disciplinary Breakthrough Project of Ministry of Education (MOE, #00975101), the Tianchi Talent Introduction Program of Xinjiang Autonomous Region, China (2023- "2 + 5"), and the Tingzhou Talent Introduction Program of Changji Autonomous Region, China (2023). This work has received funding from The National Key Research and Development Program of China (2021YFD1900200), the Program of Advanced Discipline Construction in Beijing (Agriculture Green Development), and the 2115 Talent Development Program of China Agricultural University to C.-X. S.

Author contributions

Y.-M.Z., S.-H.G., and C.-X.S. conceptualized and designed the research. Q.-F.L., K.-G.W., and S.-H.G. performed the most of experiment, methodology, data analysis and curation, and J.M., D.-M.C., Z.-G.C., B.-S.L., X.-Y.Z., N.-Q.W., T.-Q.W., and Z.-C.D. performed most of the experiments in the field and greenhouse. Q.F.L., S.-H.G., K.-G.W., F.-S.Z., J.M.R., S.G., C.-X.S., and Y.-M.Z. wrote and revised the manuscript. All authors discussed the results and commented on the manuscript. Y.-M.Z. supervised the study.

Competing interests

The authors declare no competing interests.

Additional information

Supplementary information The online version contains supplementary material available at https://doi.org/10.1038/s41467-026-69647-y.

Correspondence and requests for materials should be addressed to Shaohua Gu, Chunxu Song or Yuanmei Zuo.

Peer review information *Nature Communications* thanks Lingfei Hu, and the other, anonymous, reviewer(s) for their contribution to the peer review of this work. A peer review file is available.